# Size Distribution, Seasonal Variations and Sources of Carbonaceous Aerosol in a Typical Industrial City Nanjing in Yangtze River Delta, China

Honglei Wang[1*], Junlin An[1], Bin Zhu[1], Lijuan Shen[2], Qing Duan[3], Yuanzhe Shi[1]

1. Collaborative Innovation Center on Forecast and Evaluation of Meteorological Disasters，Key Laboratory for Aerosol-Cloud-Precipitation of China Meteorological Administration, Nanjing University of Information Science and Technology, Nanjing 210044, China;
2. Jiaxing Environmental Monitoring Station, Jiaxing 314000, China
3. Fujian Provincial Meteorological Bureau, Fuzhou 350001, China

*Corresponding author: hongleiwang@nuist.edu.cn

**Highlight:**

1. The size distribution and seasonal character of carbonaceous aerosols was provided.
2. OC, EC, SOC and POC in four seasons were mainly centralized in $PM_{1.1}$
3. Emission sources were discussed as reasons for OC/EC size distribution and seasonal variation

**Abstract:** In order to investigate the size distributions and seasonal variations of carbonaceous aerosols (OC and EC), the carbonaceous species were collected and then analyzed by using a 9-stage Anderson-type aerosol sampler and DRI Model 2001A Thermal/Optical Carbon Analyzer on the typical industrial city Nanjing in Yangtze River Delta, China in the summer, autumn and winter of 2013 and spring of 2014. OC, EC, SOC and POC exhibited obvious seasonal variations, with the highest level in winter (39.1±14.0, 5.7±2.1, 23.6±11.7 and 14.1±5.7 $\mu g \cdot m^{-3}$) and the lowest level in summer (20.6±6.7, 3.3±2.0, 12.2±3.8 and 8.4±4.1 $\mu g \cdot m^{-3}$), and were mainly centralized in $PM_{1.1}$ in four seasons. The concentrations of OC in $PM_{1.1}$ varied in the order of winter > autumn > spring > summer, while EC ranked in the order of autumn > winter > summer > spring. In the $PM_{1.1\text{-}2.1}$ and $PM_{2.1\text{-}10}$, the concentrations of OC and EC decreased in the sequence of winter > spring > autumn > summer. The size spectra of OC, EC and SOC had bimodal distributions in four seasons, except for EC with four peaks in summer. The size spectra of POC varied greatly with seasons, exhibiting bimodal distribution in winter, trimodal distribution in spring and summer, and four peaks in autumn. The OC/EC ratios were 7.0, 6.3, 7.6 and 6.9 in spring, summer, autumn and winter, respectively, which demonstrated the abundance of secondary organic aerosols in Nanjing. The sources of carbonaceous aerosol varied significantly with seasons, and were dominated by vehicle exhaust, coal and biomass burning in $PM_{2.1}$, and dominant by dust, coal and biomass burning in $PM_{2.1\text{-}10}$.

**Keyword:** size distribution; OC; EC; seasonal variation; Yangtze River Delta

## 1. Introduction

Carbonaceous aerosol fractions, accounting for 10-50 % of the PM concentration, play a key role in visibility, human health, Earth's radiation balance and cultural heritage (Cao et al., 2005, 2009a, 2015; Chow et al., 2002a, 2009; Jaffrezo et al., 2005; Ramanathan et al., 2008; Seinfeld and Pandis, 2012; Turpin et al., 1995, 2001). Carbonaceous aerosols are generally divided into organic carbon (OC), elemental carbon (EC) and inorganic carbonate carbon (CC). The OC are normally generated from primary and secondary sources, while EC originate mainly from incomplete fuel combustions of industrial boilers/kilns and residential stoves, iron and steel production, and vehicles (Cao et al., 2005; Wang et al., 2015). Previous studies also observed that both OC and EC can be formed from emissions of coal, fossil fuels, biomass, and industrial activities (Cao et al., 2003; Park et al., 2011).

At present, it has been extensively studied for the characteristics of carbonaceous aerosols in the worldwide, including their mass concentration and sources (Cao et al., 2003, 2005; Castro et al., 1999; Chen et al., 2006; Chow et al., 2002b; Duan et al., 2005; Ho et al., 2006; Pandis et al., 1993; Turpin et al.,1991; Wang et al., 2015), seasonal and spatial variations (Li et al., 2015; Philip et al., 2014; Zhang et al., 2011), size distributions (Jaffrezo et al., 2005; Lan et al., 2011; Li et al., 2012; Turpin et al.,1990, 1995, 2001; Wan et al., 2015), impacts on visibility (Andreae et al., 2008; Chow et al., 2009), connections with meteorological conditions (Cao et al., 2009b; Chow et al.,1995; Ni et al., 2015) and transformation mechanisms (Andreae et al., 2001; Castro et al., 1999; Ho et al., 2006). Andreae et al. (2001) and Li et al. (2015) revealed that the OC proportion contributed by biomass burning can be calculated by using the mass concentration ratio of OC and $K^+$. Related researches investigated that the OC/EC ratio could be used to determine the sources of the carbonaceous aerosols in the atmosphere (Chen et al., 2006; He et al., 2004; Schauer et al., 1999, 2002; Zhang et al., 2007).

With the rapid growth of China's economy and urbanization, the carbonaceous aerosols are proved to be one of the major pollutants in China (Lu et al., 2011; Zhang et al., 2012). As one of the three major regions in eastern China (Yangtze River Delta, Beijing-Tianjin-Hebei and Pearl River Delta), the YRD has been suffering the highest aerosol concentrations and the longest pollution episodes (Cao et al., 2003; Duan et al., 2007; Li et al., 2015; Wang et al., 2013, 2014). The organic matter (OM) and black carbon (BC) in $PM_1$ was estimated to be 32.1 and 9.1 % in

summer, and 30.3 and 16.9 % in winter, respectively in the YRD (Huang et al., 2013). Cao et al. (2009a) reported the annual sum concentration of OC and EC was 25.5 $\mu g \cdot m^{-3}$ and constituted about 28.5 % in $PM_{10}$ in Hangzhou. Li et al. (2015) found the mass fraction of the total carbonaceous aerosol (TCA) in $PM_{2.5}$ was estimated to be 23 % in Nanjing. Feng et al. (2009) calculated the total amount of OC and EC was in the range of 17.5-20.4 $\mu g \cdot m^{-3}$ and TCA contributed about 30 % of $PM_{2.5}$ in Shanghai. In 2010, emissions of three major $PM_{2.5}$ species in the YRD, namely OC, EC and sulfate, are 136.9 kt, 75.0 kt and 76.2 kt, respectively (Fu et al., 2013). Hou et al. (2011) demonstrated that concentrations of OC and EC on haze days were 1.5-3.9 times higher than those on clean days in Shanghai. However, these studies were mainly centralized in the characteristics of carbonaceous aerosols in $PM_{2.5}$ or $PM_{10}$ with few concerns about their size distributions in different seasons. An understanding of the size distribution characteristics of EC and OC is essential when studying the aerosol sources, light extinction, and their effects on regional and global climate and human health (Lan et al., 2011; Park et al., 2011; Wan et al., 2015). In this study, the size distributions of carbonaceous aerosols (OC and EC) over different seasons were collected and further analyzed by using a 9-stage Anderson-type aerosol sampler and DRI Model 2001A Thermal/Optical Carbon Analyzer on the typical industrial city Nanjing in Yangtze River Delta, China. We also calculated the concentrations of secondary organic carbon (SOC) and primary organic carbon (POC). This paper reported the concentration levels and the seasonal variations of these measured species. Furthermore, we discussed the carbonaceous aerosol sources in different size segment in four seasons. It is important to analyze the size distribution of OC, EC, OC/EC ratios and SOC for better understanding the sources, formation mechanisms, and control strategy of carbonaceous aerosols in the typical polluted city.

## 2. Instruments and Experiments

### 2.1 Observation stations and experiment descriptions

The observation site was located on the meteorology building (32.21ºN, 118.72ºE) of the Nanjing University of Information Science & Technology campus, which is 40 m above the ground. The information of the station and its' surroundings is shown in Figure 1. The Nanjing Chemical Industry Park (NCIP) is located at approximately 3 km of the measurement site. In addition, there are some iron and steel plants and cogeneration power plants in the range of 1 km from the site. This region represents a combination of traffic, urban, industry and croplands

sources.

The measurements were carried out during Apr 17 to May 22, 2014 (spring), Jun 1 to Jul 17, 2013 (summer), Oct 15 to Nov 13, 2013 (autumn) and Dec 30, 2013 to Jan 23, 2014 (winter) (table1). Main meteorological factors' changes were recorded by automatic weather station. The size-segregated aerosol particles were continuously collected for 23 h. After excluding the invalid data, 135 samples were obtained during the observation period, there were 36, 44, 30 and 25 samples in spring, summer, autumn and winter, respectively. Every sample contained data about OC and EC particles in 9 size segments in $PM_{10}$. The YRD region belongs to subtropical monsoon climate, which is generally prevailed by southeast wind, high temperature and abundant precipitation in summer. The average temperature and RH in summer were 26.4±4.5 °C and 67.3±16.2 %, respectively (Table 1). Table 1 also shows that the RH in four seasons were higher than 50%, the wind speed were large in spring and summer, and small in autumn and winter.

Table 1 Observation period and major meteorological elements in Nanjing

| | Observation period | Temperature(°C) | RH(%) | Wind speed($m \cdot s^{-1}$) |
|---|---|---|---|---|
| spring | 2014.4.17-5.22 | 19.2±4.3 | 61.5±22.1 | 2.2±1.2 |
| summer | 2013.6.1-7.17 | 26.4±4.5 | 67.3±16.2 | 2.5±1.1 |
| autumn | 2013.10.15-11.13 | 15.0±3.7 | 63.4±18.1 | 1.8±1.1 |
| winter | 2013.12.30-2014.1.23 | 5.0±3.7 | 53.2±21.8 | 1.9±1.0 |

**2.2 Instrumentation**

The sampling observations were carried out by a 9-stage Anderson-type aerosol sampler (Anderson 2000 Inc., USA) with size ranges of <0.43, 0.43-0.65, 0.65-1.1, 1.1-2.1, 2.1-3.3, 3.3-4.7, 4.7-5.8 5.8-9.0 and 9.0-10.0 μm for carbonaceous aerosols. The flow rate required by the Anderson-type aerosol sampler is 28.3 L/min. The sampler was operated with a 81 mm Quartz fiber filters (Whatman, Clifton, England), and the filters were baked at 800 °C for 4 h before sampling in order to minimize the background of organic carbon.

OC and EC collected by Quartz filter were then analyzed with a DRI Model 2001A Thermal/Optical Carbon Analyzer, using the IMPROVE_A (Interagency Monitoring of Protected Visual Environments) protocol (Chow et al., 2001) to measure the carbon fractions. The filter was heated stepwise to 140 °C, 280 °C, 480 °C, and 580 °C in a pure helium environment to determine OC1, OC2, OC3 and OC4, respectively. Consequently, the filter was heated to 580 °C, 740 °C and 840 °C in 2 % $O_2$ / 98 % He to determine EC1, EC2 and EC3, respectively. One sample was

selected at random from every 10 samples to carry out a duplicate sample analysis. The errors in the measurement presented here were less than 10% for TC. Field blanks were used to determine any possible background contamination; the OC and EC concentrations in the field blanks were less than 1 % of the sample levels.

For calibration and quality control, measurement with prefired filter blank, standard sucrose solution and replicate analysis were performed. Field blank samples were collected in each season and their concentration levels of OC and EC were 0.5-0.7 and 0-0.03 μg·cm$^{-2}$, less than 3 % and 1 % of the samples, respectively. The samples were corrected by each field blank samples. The detect limit for OC and EC is 0.45 μg·cm$^{-2}$ and 0.06 μg·cm$^{-2}$, respectively. More information about the instruments (e.g., precision and calibration) and the methods of data quality control were reported by Cao et al. (2003), Chow et al. (2001, 2002a), Han et al. (2007) and Li et al. (2012, 2015).

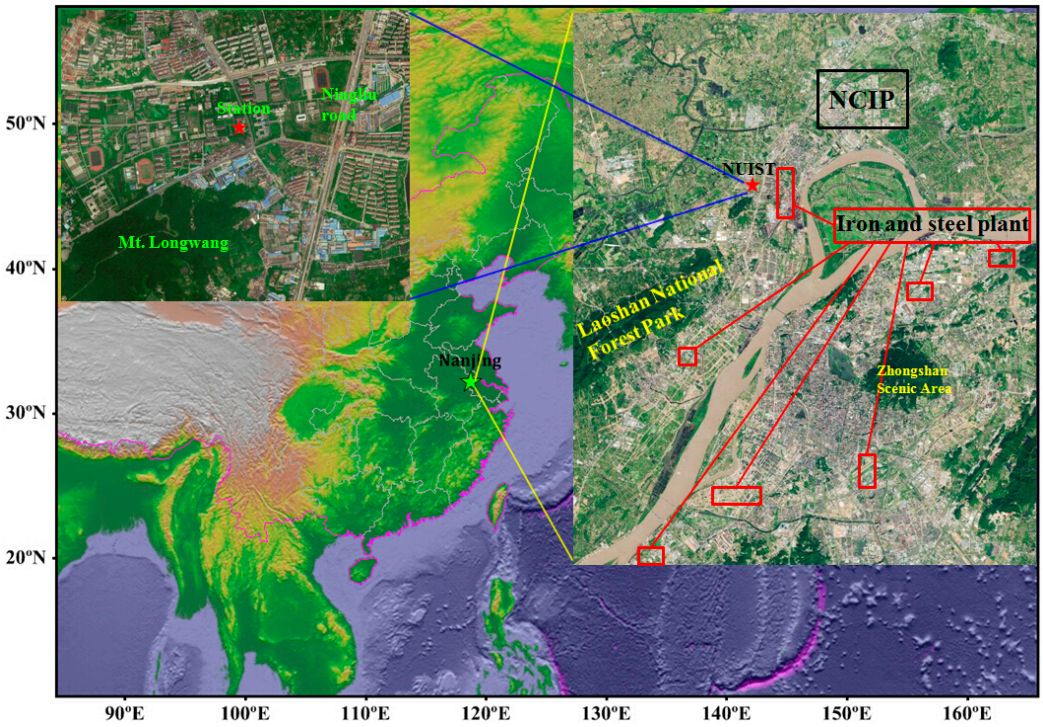


Figure 1 Location of sampling site in Nanjing

## 3. Results and discussion

### 3.1 Seasonal variations of the carbonaceous aerosol

Fig. 2a exhibits that the seasonal variations of OC ranked in the order of winter (39.1 $\mu g \cdot m^{-3}$) > autumn (30.5 $\mu g \cdot m^{-3}$) > spring (25.2 $\mu g \cdot m^{-3}$) >summer (20.6 $\mu g \cdot m^{-3}$) in Nanjing, which was similar to that of EC, who had the average concentrations of 3.6, 3.3, 4.0 and 5.7 $\mu g \cdot m^{-3}$ in spring, summer, autumn and winter according to Fig. 2b. This phenomenon might be attributed to the monsoon effects, the air masses in summer were clean due to winds majorly from the southeast ocean area. In winter, the air masses were mainly from inland area and carried amounts of pollutants attributed to the dominant northwest wind.

The concentrations of OC and EC in four seasons were mainly centralized in fine particles (Fig. 2), the proportions of which in $PM_{2.1}$ to the total mass concentration were 59.1-69.2 % and 51.2-71.9 %, and were 43.6-54.3 % and 34.5-58.7 % for the proportion in $PM_{1.1}$. The clear enrichment of carbonaceous composition in smaller particle size, particularly for EC, indicates the important roles of certain combustion sources of anthropogenic origin, from which OC and EC were confirmed to be concentrated in fine particles (Li et al., 2007, 2015).

The maximum values of OC were located at 0.65-1.1 μm in spring, autumn and winter, accounting for 18.9 %, 19.9 % and 21.6 % of the total concentration, respectively. In summer, the maximum value of OC was located at 0-0.43 μm, accounting for 19.8 % of the total concentration. The maximum value of EC was located at 1.1-2.1 μm in spring and winter and at 0-0.43 μm in summer and autumn, accounting for 20.3 %, 16.8 %, 32.7 % and 23.0 % of the total concentration, respectively.

Table 2 shows that the seasonal variations of OC and EC were quite different in $PM_{1.1}$, while were unanimous in $PM_{1.1\text{-}2.1}$ and $PM_{2.1\text{-}10}$. The concentrations of OC and EC in $PM_{1.1}$ varied in the order of winter > autumn > spring >summer, and autumn > winter > summer >spring. In the $PM_{1.1\text{-}2.1}$ and $PM_{2.1\text{-}10}$, the concentrations of OC and EC varied identically in the order of winter > spring > autumn > summer.

Table 2 Concentrations of OC, EC, SOC and POC in $PM_{1.1}$, $PM_{1.1\text{-}2.1}$ and $PM_{2.1\text{-}10}$

| | | spring | summer | autumn | winter |
|---|---|---|---|---|---|
| $PM_{1.1}$ | OC(μg·m$^{-3}$) | 11.0±3.9 | 9.8±3.9 | 16.6±7.2 | 19.7±7.7 |
| | EC(μg·m$^{-3}$) | 1.5±0.8 | 1.9±0.7 | 2.2±1.4 | 2.0±1.1 |
| | SOC(μg·m$^{-3}$) | 6.3±3.1 | 5.3±2.8 | 11.2±6.3 | 12.6±7.4 |
| | POC(μg·m$^{-3}$) | 4.1±2.0 | 4.4±1.8 | 4.9±2.4 | 6.4±3.5 |
| $PM_{1.1\text{-}2.1}$ | OC(μg·m$^{-3}$) | 4.2±1.9 | 2.4±1.0 | 4.0±2.0 | 7.4±5.4 |
| | EC(μg·m$^{-3}$) | 0.7±0.5 | 0.4±0.3 | 0.5±0.4 | 1.0±0.6 |
| | SOC(μg·m$^{-3}$) | 1.4±1.5 | 1.5±0.7 | 2.0±1.5 | 4.2±5.2 |
| | POC(μg·m$^{-3}$) | 2.0±1.4 | 0.9±0.5 | 1.8±1.2 | 3.0±2.0 |
| $PM_{2.1\text{-}10}$ | OC(μg·m$^{-3}$) | 10.0±2.9 | 8.4±3.1 | 9.9±3.5 | 12.1±3.7 |
| | EC(μg·m$^{-3}$) | 1.4±0.9 | 0.9±0.8 | 1.3±0.8 | 2.8±1.5 |
| | SOC(μg·m$^{-3}$) | 6.2±2.4 | 5.2±1.5 | 6.4±2.5 | 6.8±2.6 |
| | POC(μg·m$^{-3}$) | 3.5±2.2 | 3.0±2.7 | 3.2±1.9 | 4.7±2.4 |

The concentrations of OC in $PM_{1.1\text{-}2.1}$ were almost unanimous in spring and autumn, as a result of frequent biomass burning processes in the two seasons. It was observed that the biomass burning mainly affected aerosol chemical composition at 1.1-2.1 μm (Pósfai et al., 2003; Wang et al, 2012). The concentrations of OC in $PM_{1.1\text{-}2.1}$ was 7.4 μg·m$^{-3}$ in winter and was 3.1 times larger than summer. This phenomenon was mainly because of stable boundary layer and few precipitations in winter, besides, haze events occurred frequently as well.

**3.2 Size distributions of carbonaceous aerosol**

Fig.3a shows that the size spectra of OC had bimodal distributions in four seasons. The highest peak appears in the size range of 0.43-0.65 μm except for spring and the second peak is located at 4.7-5.8 μm. It should be pointed out that the highest peak in spring was observed to shift to a larger size (i.e. 0.65-1.1 μm).

The peak at 0.43-0.65 μm for OC was normally formed by the condensation and coagulation growth process of fine particles (gas-to-particle) (Jaffrezo et al., 2005; Miguel et al., 2004; Seinfeld and Pandis, 2012). The larger peak at 4.7-5.8 μm appeared to be related to the dust particles, which provide surfaces for the uptake of gas species and serves as a carrier for carbonaceous constituents (Seinfeld et al., 2004). In addition, the biogenic aerosols, such as algae, pollen, vegetation debris, virus, and microorganisms may be responsible for the second peak as well (Wan et al., 2015).

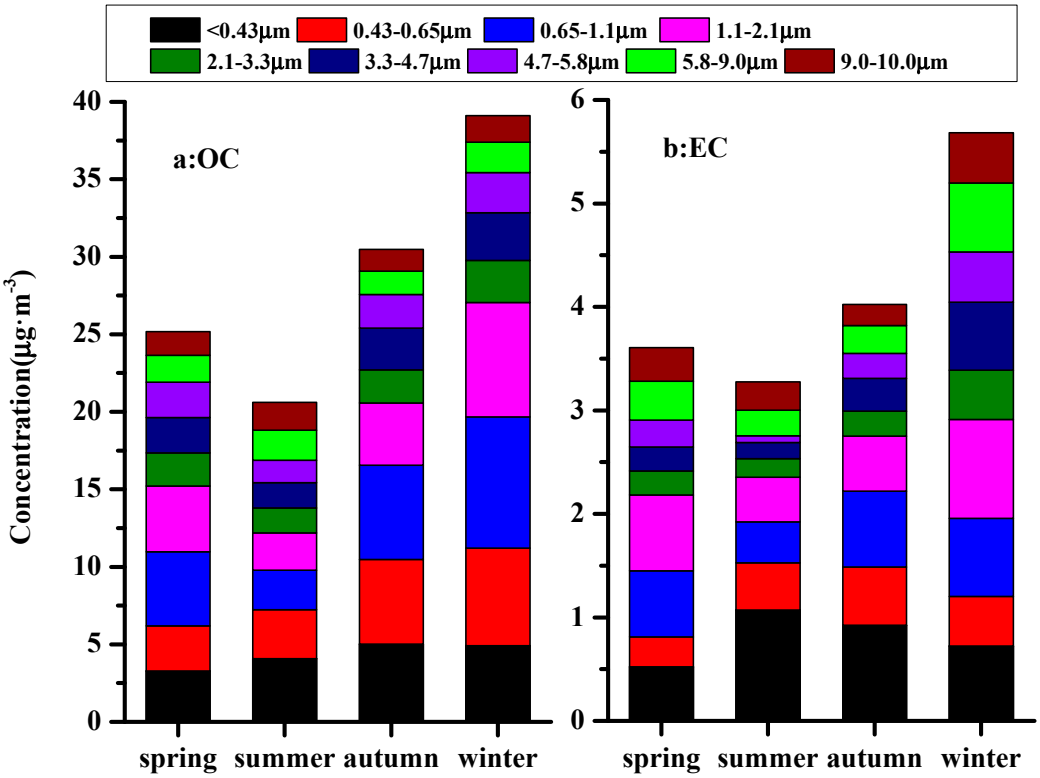


Figure 2 Size distributions of OC and EC mass concentration in four seasons

EC also presents bimodal distributions with first peak locating at 1.1-2.1 μm, 0.65-1.1 μm and 1.1-2.1 μm in spring, autumn and winter according to Fig. 3b. The second peak is unanimously lied at 4.7-5.8 μm. Fine EC particles mainly comes from vehicle exhaust, industrial emissions and coal and biomass combustion process (Cao et al., 2005; Kupiainen et al., 2007; Wang et al., 2015). The EC peak at 4.7-5.8 μm may be related to the re-suspension of EC-containing soil/dust particles (Lan et al., 2011). However, the size spectra of EC had four peaks in summer (Fig. 3b) locating at 0.5, 1.6, 4.0 and 7.4 μm, respectively. The reason is not clear, and may be associated with subway construction at Ningliu road during observation period.

Preprints (www.preprints.org) | NOT PEER-REVIEWED | Posted: 1 March 2017 doi:10.20944/preprints201703.0010.v1

Peer-reviewed version available at Atmosphere 2017, 8, , 73; doi:10.3390/atmos8040073

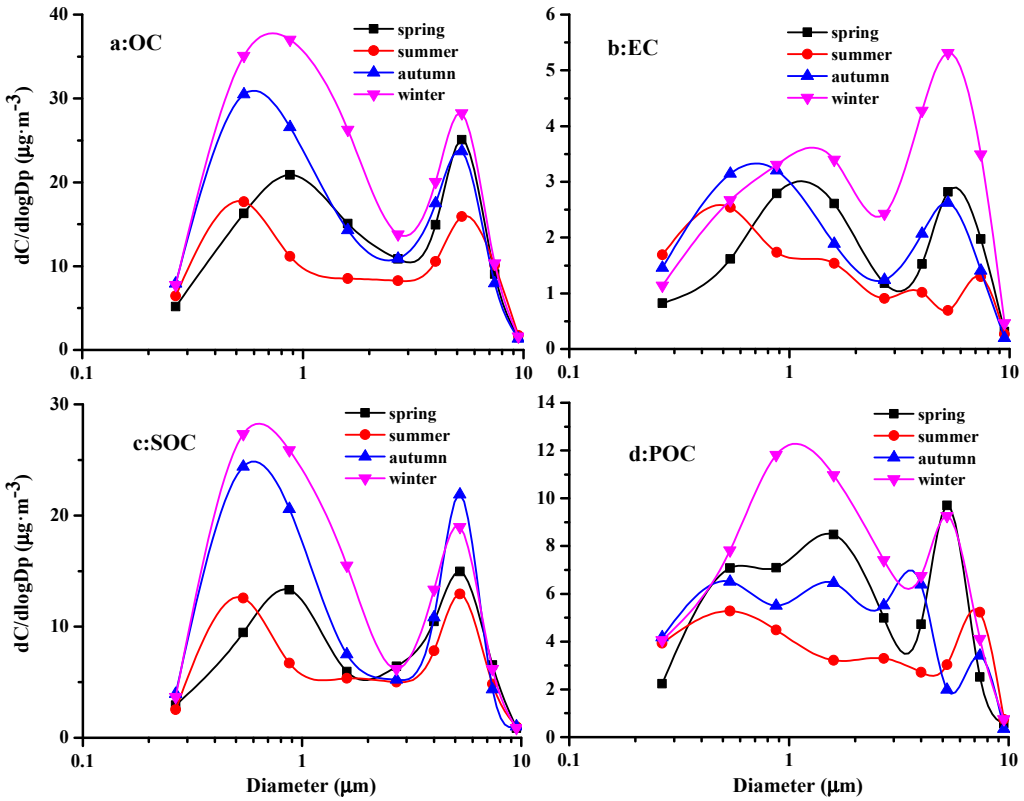


Figure 3 Spectral distributions of OC, EC, SOC and POC mass concentration in four seasons

The roles of secondary organic aerosol (SOC) in haze, visibility, climate, and heath has been recognized for decades (Cao et al., 2003; Chow et al., 1995; Gentner et al., 2012; Li et al., 2012, 2015). As shown in Table 3, most ratios of the minimum valve of OC/EC concentrations in four seasons are above 2.0, indicating that the SOC were considered to be formed in the observation period. For the control of particulate pollution, it is very crucial to quantify the contributions of the primary and secondary organic carbon to carbonaceous aerosol. However, there is no simple direct analytical technique to attain the evaluation of SOC formation in ambient aerosols, several indirect methodologies have been applied (Cao et al., 2003; Castro et al., 1999; Huang et al., 2012; Pandis et al., 1993; Turpin et al., 1991). According to Castro et al. (1999), the production of SOC can be calculated from the following equation: $SOC = OC - EC \times (OC/EC)_{\min}$

where SOC is the secondary OC, and $(OC/EC)_{\min}$ is the minimum ratio observed. We calculated the SOC concentration in 9 size segments in four seasons based on the values of $(OC/EC)_{\min}$ as shown in table 3.

Table 3 the minimum valve of OC/EC concentrations at the four seasons

| Diameter(μm) | 0~0.43 | 0.43~0.65 | 0.65~1.1 | 1.1~2.1 | 2.1~3.3 | 3.3~4.7 | 4.7~5.8 | 5.8~9.0 | 9.0-10 |
|---|---|---|---|---|---|---|---|---|---|
| spring | 2.83 | 4.53 | 3.03 | 4.00 | 4.29 | 3.09 | 3.73 | 1.35 | 1.99 |
| summer | 2.35 | 2.12 | 2.65 | 2.14 | 3.73 | 2.88 | 4.70 | 4.14 | 2.88 |
| autumn | 2.81 | 2.20 | 2.08 | 3.73 | 4.72 | 3.39 | 0.97 | 2.67 | 1.82 |
| winter | 3.70 | 3.32 | 3.69 | 3.35 | 3.23 | 1.70 | 1.89 | 1.25 | 1.69 |

The concentrations of SOC in $PM_{1.1}$ and $PM_{2.1\text{-}10}$ varied identically in the order of winter > autumn > spring > summer, and varied in the order of winter > autumn > summer > spring in $PM_{1.1\text{-}2.1}$ (table 2). The proportions of SOC in $PM_{1.1}$, $PM_{1.1\text{-}2.1}$ and $PM_{2.1\text{-}10}$ to the total concentration were 44.1-57.1 %, 10.4-17.7 % and 28.9-43.6 %, respectively. The formation mechanism of SOC is not clear at present, which is generally considered to be from gas phase reactions followed by gas-to-particle conversion of products, i.e., through nucleation, condensation, and/or sorption, perhaps followed by aerosol phase reactions (Castro et al., 1999; Gentner et al., 2012).

The concentrations of POC in $PM_{1.1}$ ranked in the order of winter > autumn > summer > spring, and in the order of winter > spring > autumn> summer in $PM_{1.1\text{-}2.1}$ and $PM_{2.1\text{-}10}$ (table 2). POC in $PM_{1.1}$ was the highest in winter (6.4 $\mu g \cdot m^{-3}$) and were unanimous in the rest three seasons (4.1-4.9 $\mu g \cdot m^{-3}$). POC in $PM_{1.1\text{-}2.1}$ varied greatly with seasons, and had the highest level in winter (3.0 $\mu g \cdot m^{-3}$) and lowest level in summer (0.9 $\mu g \cdot m^{-3}$). The concentrations of POC in $PM_{2.1\text{-}10}$ were almost unanimous in all seasons, the value of which in winter (4.7 $\mu g \cdot m^{-3}$) was slightly higher than other seasons (3.0-3.5 $\mu g \cdot m^{-3}$). POC are mainly from direct emissions of combustion process, and mostly centralized in fine particles. POC in coarse particles are observed to be mainly from the emission of plant spores and pollen, vegetation debris, tire rubber and soil organic matter wind erosion and some non-combustion industrial activities (Chow et al., 1995; Schauer et al., 1996).

The size spectra of SOC had bimodal distributions in four seasons as shown in Fig.3c, which were similar to OC. While the size spectra of POC changed greatly with seasons. POC had bimodal distribution in winter peaking at 0.65-1.1 μm and 4.7-5.8 μm, and had trimodal size distribution in spring and summer, peaking at 0.43-0.65 μm, 1.1-2.1 μm and 4.7-5.8 μm in spring, and at 0.43-0.65 μm, 2.1-3.3 μm and 5.8-9.0 μm in summer. In autumn, the spectra of POC had four peaks at 0.43-0.65 μm, 1.1-2.1 μm, 3.3-4.7 μm and 5.8-9.0 μm.

### 3.3 Source analysis of OC and EC

#### 3.3.1 Relationships between OC and EC

The relationships between OC and EC can provide valuable information for the source origins of carbonaceous aerosols (Turpin et al., 1990, 1995). Strong correlation indicates common source origins and transport process. Fig. 4a shows that the correlation coefficients of OC with EC were the highest in summer (0.73), followed by spring (0.54) and autumn (0.52), and the lowest in winter (0.25). The strong correlations between OC and EC in spring, summer and autumn samples suggested that they were derived largely from the similar sources, opposite to those in winter. Meanwhile, the correlation coefficients between OC and EC varied greatly with seasons in $PM_{1.1}$, $PM_{1.1\text{-}2.1}$ and $PM_{2.1\text{-}10}$. In $PM_{1.1}$, the correlations were observed to be large in spring (0.60) and summer (0.76), and low in autumn (0.44) and winter (0.32) according to Fig. 4b. In $PM_{1.1\text{-}2.1}$, the correlation coefficients were high in spring (0.60), summer (0.70) and autumn (0.64), and low in winter (0.36) (figure 4c). In $PM_{2.1\text{-}10}$, the correlation coefficients were high in all seasons (0.54-0.87). It can be seen that source emissions of OC and EC in fine particles had greatly seasonal variations, whereas they had the common sources in coarse particles.

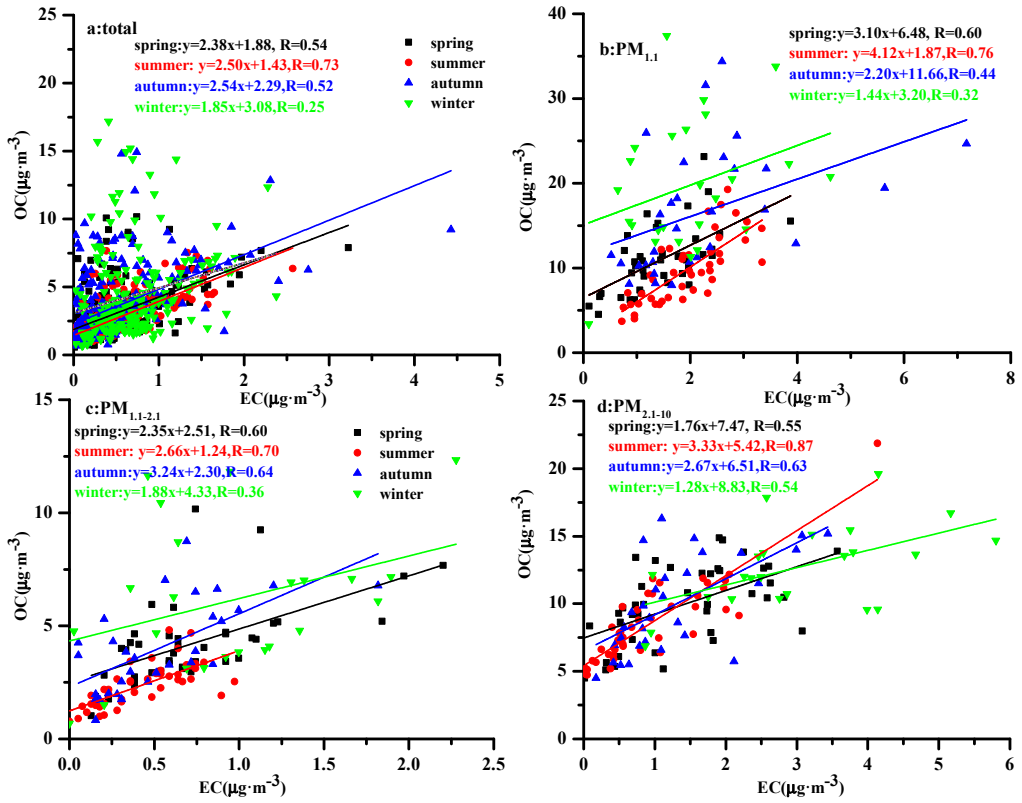


Figure 4 The relationships between OC and EC in four season at Nanjing

### 3.3.2 Implications of the OC/EC ratios

The ratio of OC/EC is an important diagnostic index that has been used to reflect the type and source strength of carbonaceous aerosols (Turpin and Lim, 2001). The ratios can be mainly affected by emission sources, secondary organic aerosol (SOA) formation, and different removal rates by deposition (Cachier et al., 1996). The OC/EC ratios exceeding 2.0 have been used to indicate the presence of secondary organic aerosols (Cao et al., 2005; Chow et al., 2006; Turpin and Huntzicker, 1995); 1.0-4.2 indicate diesel and gasoline vehicle exhaust emissions (Schauer et al., 1999, 2002), 2.4-14.5 indicate biomass burning emissions (Ram et al., 2010), 2.5-10.5 indicate coal combustion emissions (Chen et al., 2006), 32.9-81.6 indicate cooking emissions (He et al., 2004). Watson et al. (1994) reported the OC/EC ratio of 13.1 for dust emissions.

Fig. 5 reveals that the ratio of OC/EC exceeded 2 in all seasons, which demonstrated the abundance of SOC in Nanjing. The spectra of OC/EC had bimodal distributions in spring and summer. The two peaks were located at 0.43-1.1 μm and 2.1-5.8 μm in spring, with values of 18.0 and 14.0, respectively. Therefore, the sources of carbonaceous species in fine particles may originate from coal and biomass burning, and from coal and biomass burning and dust emissions in coarse particles. Besides, long-range transport from northern area was another important source of carbonaceous aerosols in Nanjing. The values of OC/EC in < 2.1 μm were 4.2-9.4 in summer, suggesting their sources from vehicle exhaust, coal and biomass burning emissions. The value of OC/EC in the coarse particles varied greatly with sizes in summer, with the highest peak value of 26.9 at 4.7-5.8 μm, the lowest value of 8.8 at 9-10 μm, suggesting that the sources were from dust, coal and biomass burning.

The spectra of OC/EC had trimodal distributions in autumn and winter (Fig. 5). The peak at 0.43-1.1 μm had the highest value of 26.9-33.1 in autumn, suggesting cooking emission sources. The value of OC/EC in <0.43 μm was 5.7 for vehicle exhaust emissions; 13.0-13.8 at 1.1-4.7 μm for dust and coal and biomass burning. The peak values at 4.7-5.8 μm and 9.0-10 μm were 19.1 and 16.2, mainly from biomass burning. In winter, the values of OC/EC were 5.3-6.4 in <0.65 μm, indicated vehicle exhaust and coal combustion; 12.0-20.8 at 0.65-2.1 μm indicated coal and biomass burning, 2.1-7.3 at 2.1-10 μm indicated vehicle exhaust and coal combustion.

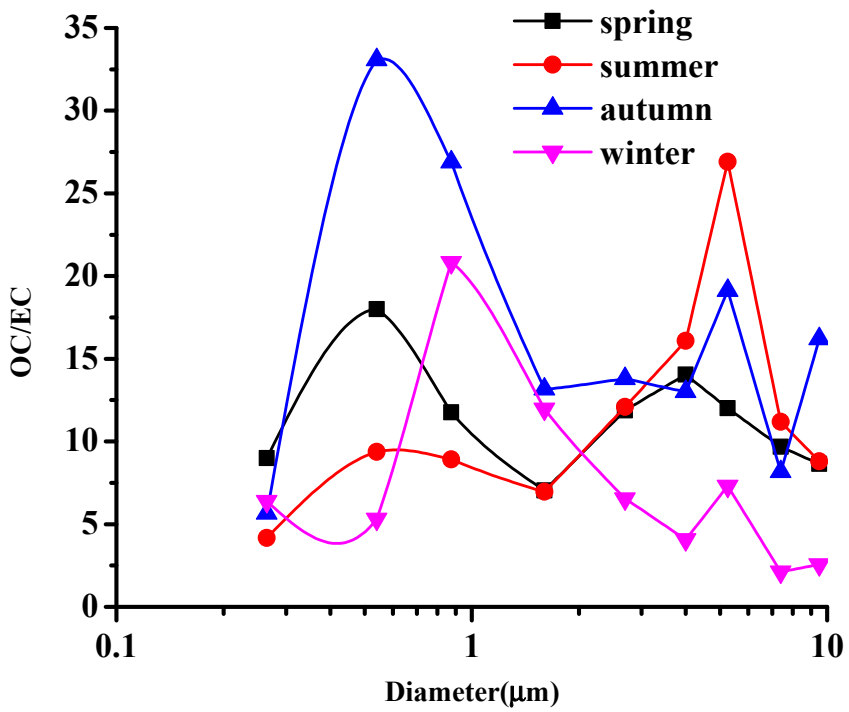


Figure 5 Spectral distributions of OC/EC in four seasons

**4 Conclusions**

In order to investigate the size distributions and seasonal variations of carbonaceous aerosols (OC and EC), the carbonaceous species were observed at the typical industrial city Nanjing in Yangtze River Delta, China. OC, EC, SOC and POC exhibited obviously seasonal variations, with the highest level in winter (39.1±14.0, 5.7±2.1, 23.6±11.7 and 14.1±5.7 $\mu g \cdot m^{-3}$) and the lowest level in summer (20.6±6.7, 3.3±2.0, 12.2±3.8 and 8.4±4.1 $\mu g \cdot m^{-3}$). The OC, EC, SOC and POC in four seasons were mainly centralized in $PM_{1.1}$, with the proportions in the range of 34.5-58.7 %. OC concentrations at 0.65-1.1 μm were the highest in spring, autumn and winter, and the lowest at 0-0.43 μm in summer. The EC maximum values were located at 1.1-2.1 μm in spring and winter, and at 0-0.43 μm in summer and autumn, respectively. The concentrations of OC and EC in $PM_{1.1}$ varied in the order of winter > autumn > spring > summer, and autumn > winter > summer > spring. In the $PM_{1.1\text{-}2.1}$ and $PM_{2.1\text{-}10}$, the concentrations of OC and EC ranked uniformly in the order of winter > spring > autumn > summer.

The size spectra of OC, EC and SOC had bimodal distributions in four seasons, except for EC with four peaks in summer. However, the size distributions of OC, EC and SOC in fine particles are a little complex in four seasons. The size spectra of POC varied greatly with seasons,

exhibiting bimodal distribution in winter, trimodal distribution in spring and summer, and four peaks in autumn.

The correlation coefficients between OC and EC were the highest in summer (0.73), followed by spring (0.54) and autumn (0.52), and the lowest in winter (0.25), indicating their common emission sources in spring, summer and autumn. The correlation coefficients of OC with EC varied greatly with seasons in $PM_{1.1}$, $PM_{1.1\text{-}2.1}$ and $PM_{2.1\text{-}10}$. Strong correlations between OC and EC were observed in spring (0.60) and summer (0.76) in $PM_{1.1}$, in spring (0.60), summer (0.70) and autumn (0.64) in $PM_{1.1\text{-}2.1}$ and in all seasons (0.54-0.87) in $PM_{2.1\text{-}10}$. The ratio of OC/EC was 7.0, 6.3, 7.6 and 6.9 in spring, summer, autumn and winter, respectively, which demonstrated the abundance of secondary organic aerosols in Nanjing. The sources of carbonaceous aerosols exhibited significantly seasonal variations, which was dominated by vehicle exhaust, coal and biomass burning in $PM_{2.1}$, and by dust, coal and biomass burning in $PM_{2.1\text{-}10}$.

**Acknowledgements**

This work was supported by grants from the Chinese Academy of Sciences Strategic Priority Research Program (Grant No. XDB05020206), the Startup Foundation for Introducing Talent of NUIST(2016r040), the National Natural Science Foundation of China (grant nos. 41275143 and 41305135) and the Project Funded by the Priority Academic Program Development (PAPD) of Jiangsu Higher Education Institutions.

**References:**

Andreae, M.O., Merlet, P., 2001. Emission of trace gases and aerosols from biomass burning. Global Biogeochem. Cy., 15(4), 955-966.

Andreae, M.O., Schmid, O., Yang, H., Chand, D., Yu, J.Z., Zeng, L.M., Zhang, Y.H., 2008. Optical properties and chemical composition of the atmospheric aerosol in urban Guangzhou, China. Atmos. Environ., 42(25), 6335-6350.

Cachier, H., Liousse, C., Pertuisot, M.H., Gaudichet, A., Echalar, F., Lacaux, J.P., 1996. African fire particulate emissions and atmospheric influence. Biomass Burning and Global Change, 1(41), 428-440.

Cao, J.J., Lee, S.C., Ho, K.F., Zhang, X.Y., Zou, S.C., Fung, K., Chow, J.C., Watson, J.G., 2003. Characteristics of carbonaceous aerosol in Pearl River Delta Region, China during 2001

winter period. Atmos. Environ., 37(11), 1451-1460.

Cao, J.J., Shen, Z., Chow, J.C., Qi, G., Watson, J.G., 2009a. Seasonal variations and sources of mass and chemical composition for PM 10 aerosol in Hangzhou, China. Particuology, 7(3), 161-168.

Cao, J.J., Wu, F., Chow, J.C., Lee, S.C., Li, Y., Chen, S.W., An, Z.S., Fung, K.K., Watson, J.G., Zhu, C.S., Liu, S.X., 2005. Characterization and source apportionment of atmospheric organic and elemental carbon during fall and winter of 2003 in Xi'an, China. Atmos. Chem. Phys., 5(11), 3127-3137.

Cao, J.J., Zhu, C.S., Chow, J.C., Watson, J.G., Han, Y.M., Wang, G.H., Shen, Z.X, An, Z.S., 2009b. Black carbon relationships with emissions and meteorology in Xi'an, China. Atmos. Res., 94(2), 194-202.

Cao, J.J., Zhu, C.S., Ho, K.F., Han, Y.M., Shen, Z.X., Zhan, C.L., Zhang, J.Q., 2015. Light attenuation cross-section of black carbon in an urban atmosphere in northern China. Particuology, 18, 89-95.

Castro, L.M., Pio, C.A., Harrison, R.M., Smith, D.J.T., 1999. Carbonaceous aerosol in urban and rural European atmospheres: estimation of secondary organic carbon concentrations[J]. Atmos. Environ., 33(17), 2771-2781.

Chen, Y., Zhi, G., Feng, Y., Fu, J., Feng, J., Sheng, G., Simoneit, B.R., 2006. Measurement of Emission Factors for Primary Carbonaceous Particles from Residential Raw-Coal Combustion in China. Geophys. Res. Lett., 33(L20815), doi: 10.1029/2006GL026966.

Chow, J.C., 1995. Measurement methods to determine compliance with ambient air quality standards for suspended particles. J. Air Waste Manage., 45(5), 320-382.

Chow, J.C., Watson, J.G., 2002a. $PM_{2.5}$ carbonate concentrations at regionally representative Interagency Monitoring of Protected Visual Environment sites. J. Geophys. Res., 107(D21), DOI: 10.1029/2001JD000574.

Chow, J.C., Watson, J.G., Doraiswamy, P., Chen, L.W.A., Sodeman, D.A., Lowenthal, D.H., Park, K., Arnott, W.P., Motallebi, N., 2009. Aerosol light absorption, black carbon, and elemental carbon at the Fresno Supersite, California. Atmos. Res., 93(4), 874-887.

Chow, J.C., Watson, J.G., Edgerton, S.A., Vega, E., 2002b. Chemical composition of $PM_{2.5}$ and $PM_{10}$ in Mexico City during winter 1997. Sci. Total Environ., 287(3), 177-201.

Chow, J.C., Watson, J.G., Crow, D., Lowenthal, D.H., Merrifield, T., 2001. Comparison of IMPROVE and NIOSH carbon measurements. Aerosol Sci. Technol., 34(1), 23-34.

Duan, F., He, K., Ma, Y., Jia, Y., Yang, F., Li, Y., Tanaka, S., Okuta, T., 2005. Characteristics of carbonaceous aerosols in Beijing, China. Chemosphere, 60(3), 355-364.

Duan, J.C., Tan, J.H., Cheng, D.X., Bi, X.H., Deng, W.J., Sheng, G.Y., Fu, J.M., Wong, M.H., 2007. Sources and characteristics of carbonaceous aerosol in two largest cities in Pearl River Delta Region, China. Atmos. Environ., 41(14), 2895-2903.

Feng, Y.L., Chen, Y.J., Guo, H., Zhi, G.R., Xiong, S.C., Li, J., Sheng, G.Y., Fu, J.M., 2009. Characteristics of organic and elemental carbon in $PM_{2.5}$ samples in Shanghai, China. Atmos. Res., 92(4), 434-442.

Fu, X., Wang, S., Zhao, B., Xing, J., Cheng, Z., Liu, H., Hao, J., 2013. Emission inventory of primary pollutants and chemical speciation in 2010 for the Yangtze River Delta region, China. Atmos. Environ., 70, 39-50.

Gentner, D.R., Isaacman, G., Worton, D.R., Chan, A.W.H., Dallmann, T.R., Davis, L., Liu, S., Day, D.A., Russell, L.M., Wilson, K.R., Weber, R., Guha, A., Harley, R.A., Goldstein, A.H., 2012. Elucidating secondary organic aerosol from diesel and gasoline vehicles through detailed characterization of organic carbon emissions. P. Natl. Acad. Sci. USA, 109(45), 18318-18323.

Han, Y.M., Cao, J.J., An, Z.S., Chow, J.C., Watson, J.G., Jin, Z., Fung, K., Liu, S., 2007. Evaluation of the thermal/optical reflectance method for quantification of elemental carbon in sediments. Chemosphere 69(4), 526-533.

Han, Y.M., Cao, J.J., Lee, S.C., Ho, K.F., An, Z.S., 2010. Different characteristics of char and soot in the atmosphere and their ratio as an indicator for source identification in Xi'an, China. Atmos. Chem. Phys. 10(2), 595-607.

He, L.Y., Hu, M., Huang, X.F., Yu, B.D., Zhang, Y.H., Liu, D.Q., 2004. Measurement of Emissions of Fine Particulate Organic Matter from Chinese Cooking. Atmos. Environ. 38, 6557-6564.

Ho, K.F., Lee, S.C., Cao, J.J., Li, Y.S., Chow, J.C., Watson, J.G., Fung, K., 2006. Variability of Organic and Elemental Carbon, Water Soluble Organic Carbon, and Isotopes in Hong Kong. Atmos. Chem. Phys. 6, 4569-4576.

Hou, B., Zhuang, G., Zhang, R., Liu, T., Guo, Z., Chen, Y., 2011. The implication of carbonaceous aerosol to the formation of haze: Revealed from the characteristics and sources of OC/EC over a mega-city in China. J. Hazard. Mate. 190(1), 529-536.

Huang, H., Ho, K.F., Lee, S.C., Tsang, P.K., Ho, S., Zou, C.W., Zou, S.C., Cao, J.J., Xu, H.M., 2012. Characteristics of carbonaceous aerosol in $PM_{2.5}$: Pearl Delta River region, China. Atmos. Res. 104. 227-236.

Huang, X.F., Xue, L., Tian, X.D., Shao, W.W., Sun, T.L., Gong, Z.H., Ju, W.W., Jiang, B., Hu, M., He, L.Y., 2013. Highly time-resolved carbonaceous aerosol characterization in Yangtze River Delta of China: Composition, mixing state and secondary formation. Atmos. Environ. 64, 200-207.

Jaffrezo, J.L., Aymoz, G., Cozic, J., 2005. Size distribution of EC and OC in the aerosol of Alpine valleys during summer and winter. Atmos. Chem. Phys. 5(11), 2915-2925.

Kupiainen, K., Klimont, Z., 2007. Primary emissions of fine carbonaceous particles in Europe. Atmos. Environ. 41(10), 2156-2170.

Lan, Z.J., Chen, D.L., Li, X., Huang, X.F., He, L.Y., Deng, Y.G., Feng, N., Hu, M., 2011. Modal characteristics of carbonaceous aerosol size distribution in an urban atmosphere of South China. Atmos. Res. 100(1), 51-60.

Li, B., Zhang, J., Zhao, Y., Yuan, S., Zhao, Q., Shen, G., Wu, H., 2015. Seasonal variation of urban carbonaceous aerosols in a typical city Nanjing in Yangtze River Delta, China. Atmos. Environ. 106, 223-231.

Li, P.H., Han, B., Huo, J., Lu, B., Ding, X., Chen, L., Kong, S., Bai, Z., Wang, B., 2012. Characterization, meteorological influences and source identification of carbonaceous aerosols during the autumn-winter period in Tianjin, China. Aerosol Air Qual. Res. 12, 283-294.

Li, X., Wang, L., Wang, Y., Wen, T., Yang, Y., Zhao, Y., Wang, Y., 2012. Chemical composition and size distribution of airborne particulate matters in Beijing during the 2008 Olympics. Atmos. Environ. 50, 278-286.

Li, X., Wang, S., Duan, L., Hao, J., Li, C., Chen, Y., Yang, L., 2007. Particulate and trace gas emissions from open burning of wheat straw and corn stover in China. Environ. Sci. Technol. 41(17), 6052-6058.

Lu, Z., Zhang, Q., Streets, D.G., 2011. Sulfur dioxide and primary carbonaceous aerosol emissions in China and India, 1996-2010. Atmos. Chem. Phys. 11(18), 9839-9864.

Miguel, A.H., Eiguren-Fernandez, A., Jaques, P.A., Jaques, P.A., Froines, J.R., Grant, B.L., Mayo, P.R., Sioutas, C., 2004. Seasonal variation of the particle size distribution of polycyclic aromatic hydrocarbons and of major aerosol species in Claremont, California. Atmos. Environ. 38(20), 3241-3251.

Ni, H., Han, Y., Cao, J., Chen, L.W.A., Tian, J., Wang, X., Chow, J.C., Watson, J.G., Wang, Q., Wang, P., Li, H., Huang, R., 2015. Emission characteristics of carbonaceous particles and trace gases from open burning of crop residues in China. Atmos. Environ. 123, 399-406.

Pandis, S.N., Wexler, A.S., Seinfeld, J.H., 1993. Secondary organic aerosol formation and transport-II. Predicting the ambient secondary organic aerosol size distribution. Atmos. Environ. 27(15), 2403-2416.

Park, S.S., Cho, S.Y., 2011. Tracking sources and behaviors of water-soluble organic carbon in fine particulate matter measured at an urban site in Korea. Atmos. Environ. 45(1), 60-72.

Philip, S., Martin, R.V., Pierce, J.R., Jimenez, J.L., Zhang, Q., Canagaratna, M.R., Spracklen, D.V., Nowlan, C.R., Lamsal, L.N., Cooper, M.J., Krotkov, N.A., 2014. Spatially and seasonally resolved estimate of the ratio of organic matter to organic carbon. Atmos. Environ. 87, 34-40.

Pósfai, M., Simonics, R., Li, J., Hobbs, P.V., Buseck, P.R., 2003. Individual aerosol particles from biomass burning in southern Africa: 1. Compositions and size distributions of carbonaceous particles. J. Geophys. Res. 108(D13), doi: 10.1029/2002JD002291.

Ram, K., Sarin, M.M., 2010. Spatio-temporal variability in atmospheric abundances of EC, OC and WSOC over Northern India. J. Aerosol Sci. 41(1), 88-98.

Ramanathan, V., Carmichael, G., 2008. Global and regional climate changes due to black carbon. Nat. Geosci. 1(4), 221-227.

Schauer, J.J., Kleeman, M.J., Cass, G.R., Simoneit, B.R., 1999. Measurement of Emissions from Air Pollution Sources: 2. C1 through C30 Organic Compounds from Medium Duty Diesel Trucks . Environ. Sci. Technol. 33, 1578-1587.

Schauer, J.J., Kleeman, M.J., Cass, G.R., Simoneit, B.R., 2001. Measurement of Emissions from Air Pollution Sources: 3.C1-C29 Organic Compounds from Fireplace Combustion of Wood. Environ. Sci. Technol. 36: 1169-1180.

Schauer, J.J., Kleeman, M.J., Cass, G.R., Simoneit, B.R., 2002. Measurement of Emissions from Air Pollution Sources: 5.C1-C32 organic Compounds from Gasoline-Powered Motor Vehicles. Environ. Sci. Technol. 36, 1169-1180.

Schauer, J.J., Rogge, W.F., Hildemann, L.M., Mazurek, M.A., Cass, G.R., Simoneit, B.R., 1996. Source apportionment of airborne particulate matter using organic compounds as tracers. Atmos. Environ. 30(22), 3837-3855.

Seinfeld, J.H., Carmichael, G.R., Arimoto, R., Conant, W.C., 2004. ACE-ASIA-Regional climatic and atmospheric chemical effects of Asian dust and pollution. B. Am. Meteorol. Soc. 85(3), 367-380.

Seinfeld, J.H., Pandis, S.N., 2012. Atmospheric chemistry and physics: from air pollution to climate change. John Wiley & Sons.

Turpin, B.J., Cary, R.A., Huntzicker, J.J., 1990. An in situ, time-resolved analyzer for aerosol organic and elemental carbon. Aerosol Sci. Tech. 12(1), 161-171.

Turpin, B.J., Huntzicker, J.J., 1991. Secondary formation of organic aerosol in the Los Angeles Basin: a descriptive analysis of organic and elemental carbon concentrations. Atmos. Environ. 25(2), 207-215.

Turpin, B.J., Huntzicker, J.J., 1995. Identification of secondary organic aerosol episodes and quantitation of primary and secondary organic aerosol concentrations during SCAQS. Atmos. Environ. 29(23), 3527-3544.

Turpin, B.J., Lim, H.J., 2001. Species contributions to $PM_{2.5}$ mass concentrations: Revisiting common assumptions for estimating organic mass. Aerosol Sci. Tech. 35(1), 602-610.

Wan, X., Kang, S., Wang, Y., Xin, J., Liu, B., Guo, Y., Wen, T., Zhang, G., Cong, Z., 2015. Size distribution of carbonaceous aerosols at a high-altitude site on the central Tibetan Plateau (Nam Co Station, 4730ma. sl). Atmos. Res. 153, 155-164.

Wang, G., Cheng, S., Li, J., Lang, J., Wen, W., Yang, X., Tian, L., 2015. Source apportionment and seasonal variation of PM2.5 carbonaceous aerosol in the Beijing-Tianjin-Hebei Region of China. Environ. Monit. Assess. 187(3), 1-13.

Wang, G., Zhou, B., Cheng, C., Cao, J., Li, J., Meng, J., Tao, J., Zhang, R., Fu, P., 2013. Impact of Gobi desert dust on aerosol chemistry of Xi'an, inland China during spring 2009: differences in composition and size distribution between the urban ground surface and the mountain

atmosphere. Atmos. Chem. Phys. 13, 819-835.

Wang, H., An, J., Shen, L., Zhu, B., Pan, C., Liu, Z., Liu, X., Duan, Q., Liu, X., Wang, Y., 2014. Mechanism for the formation and microphysical characteristics of submicron aerosol during heavy haze pollution episode in the Yangtze River Delta, China. Sci. Total Environ. 490, 501-508.

Wang, H., Zhu, B., Shen, L., Kang, H., 2012. Size distributions of aerosol and water-soluble ions in Nanjing during a crop residual burning event. J. Environ. Sci. 24(8), 1457-1465.

Watson, J.G., Chow, J.C., Lu, Z., Fujita, E.M., Lowenthal, D.H., Lawson, D.R., Ashbaugh, L.L., 1994. Chemical mass balance source apportionment of $PM_{10}$ during the Southern California Air Quality Study. Aerosol Sci. Tech. 21(1), 1-36.

Zhang, F., Zhao, J., Chen, J., Xu, Y., Xu, L., 2011. Pollution Characteristics of Organic and Elemental Carbon in $PM_{2.5}$ in Xiamen, China. J. Environ. Sci. 23(8), 1342-1349.

Zhang, X.Y., Wang, Y.Q., Niu, T., Zhang, X.C., Gong, S.L., Zhang, Y.M., Sun, J.Y., 2012. Atmospheric aerosol compositions in China: spatial/temporal variability, chemical signature, regional haze distribution and comparisons with global aerosols. Atmos. Chem. Phys. 12(2), 779-799.

Zhang, Y., Shao, M., Zhang, Y., Zeng, L., He, L., Zhu, B., Wei, Y., Zhu, X., 2007. Source Profiles of Particulate Organic Matters Emitted from Cereal Straw Burnings. J. Environ. Sci. 19, 167-175.